



**HAL**  
open science

## Contributions of atmospheric plasma treatment on a hygrothermal aged carbon/epoxy 3D woven composite material

Camille Gillet, Bouchra Hassoune-Rhabbour, Fabienne Poncin-Epaillard, Tatiana Tchalla, Valérie Nassiet

### ► To cite this version:

Camille Gillet, Bouchra Hassoune-Rhabbour, Fabienne Poncin-Epaillard, Tatiana Tchalla, Valérie Nassiet. Contributions of atmospheric plasma treatment on a hygrothermal aged carbon/epoxy 3D woven composite material. *Polymer Degradation and Stability*, 2022, 202, pp.110023. 10.1016/j.polymdegradstab.2022.110023 . hal-04007207

**HAL Id: hal-04007207**

**<https://hal.science/hal-04007207v1>**

Submitted on 27 Feb 2023

**HAL** is a multi-disciplinary open access archive for the deposit and dissemination of scientific research documents, whether they are published or not. The documents may come from teaching and research institutions in France or abroad, or from public or private research centers.

L'archive ouverte pluridisciplinaire **HAL**, est destinée au dépôt et à la diffusion de documents scientifiques de niveau recherche, publiés ou non, émanant des établissements d'enseignement et de recherche français ou étrangers, des laboratoires publics ou privés.



Distributed under a Creative Commons Attribution 4.0 International License

# Contributions of atmospheric plasma treatment on a hygrothermal aged carbon/epoxy 3D woven composite material

Camille Gillet<sup>a,b,\*</sup>, Bouchra Hassoune-Rhabbour<sup>a</sup>, Fabienne Poncin-Epaillard<sup>c</sup>, Tatiana Tchalla<sup>b</sup>, Valérie Nassiet<sup>a,\*\*</sup>

<sup>a</sup>Laboratoire Génie de Production, INP-ENIT, Université de Toulouse, 47 Av. d'Azereix, 65016, Tarbes, France.

<sup>b</sup>Safran Aircraft Engines, département Matériaux et Procédés, site de Villaroche, 77550, Moissy-Cramayel, France.

<sup>c</sup>Institut des Molécules et Matériaux du Mans (CNRS n°6283), Le Mans Université, Av. Olivier Messiaen, 72085, Le Mans, France.

---

## Abstract

In this paper, the effects of hygrothermal ageing and atmospheric plasma surface treatment on a 3D carbon/epoxy-amine woven composite material are studied. The goal is to study the surface evolution of the materials in terms of chemical composition and morphology. Plasma treatment is applied on new and hygrothermally aged samples in order to analyse its contribution to the surface modifications and degradations. It appears that hygrothermal ageing has irreversible absorption behaviour causing hydrolysis, oxidation and particle losses, which modifies the surface chemistry and topology. On the other hand, the atmospheric plasma causes oxidation of the matrix. Indeed, when a repair is necessary, the damaged part could evolve due to moisture absorption related to ageing. As the fibres are exposed, the topology and surface chemistry are modified. Nevertheless, it allows to desorb the humidity adsorbed on the surface and reach an oxidation level similar to unaged treated samples.

*Keywords:* Carbon/epoxy composite, Particle migration, Hygrothermal ageing, Pre-bond ageing, Atmospheric plasma, Surface functionalization, Surface chemistry

---

## 1. Introduction

Since many decades, polymer-matrix composite materials have been widely used in many industrial applications, especially in aeronautics. Indeed, aircraft manufacturers have seen in composites the opportunity to reduce unnecessary onboard weight to impact the fossil fuel consumption of aircraft positively. They enable the replacement of metals in non-thermally exposed areas, offering excellent mechanical properties for low density. Epoxy resins are commonly used as a composite matrix or adhesive for bonded assemblies and repairs, thanks to the low density of non-crosslinked systems, which facilitates manufacturing. Several characteristics make them excellent candidates as adhesives: the presence of polar groups in their composition,

---

\*Corresponding author.

\*\*Corresponding author.

Email addresses: [camille.gillet@enit.fr](mailto:camille.gillet@enit.fr) (Camille Gillet), [valerie.nassiet@enit.fr](mailto:valerie.nassiet@enit.fr) (Valérie Nassiet)

which gives them the ability to adhere to substrates, their low shrinkage after cross-linking, and their wide cross-linking range, from 5 to over 200°C depending on their nature [1, 2].

During their lifetime, aeronautical structures can be damaged in various ways: during their manufacture, in service or during maintenance operations, and as a result of impacts. In this context of massive introduction of high value-added composite parts, structural repair becomes a key issue for the profitability of in-flight operations, complicated by the heterogeneity and anisotropy of these materials. These repairs aim to restore the initial properties of the parent structure in terms of operating performance, rigidity and safety. Therefore, various works are focused on the certification of these repair processes, which are based on the guarantee of a level of reliability equivalent to that of a healthy structure. In order to preserve the aerodynamics of the parts, adhesive repairs are expanding. They consist of replacing the damaged area with a part made of the same material as the parent structure. The distribution of mechanical stress and fatigue resistance is good, and the additional weight is very low. Besides, they require control of the assembly and its manufacturing cycle. It is a fact confirmed in several publications that good adhesive bonding and controlled surface activation on a sound structure are the guarantees of greatly improved durability under severe environmental constraints such as humidity, temperature, and acid-base environments [3–7]. Effective bonding requires a good surface condition, a contaminant-free substrate surface and a controlled roughness [8]. In bonded joints, surface treatments are very often used to increase the adhesion of the composite material substrates. They can be mechanical such as sanding and sandblasting, chemical as degreasing, or physical such as laser, atmospheric and low-pressure plasma treatment [9–12]. Atmospheric plasma treatment, in particular, has been the subject of numerous studies that have proven its interest in composite material bonding. It cleans the surface, chemically activates and in some cases alters its topology. The chemical activation of air or oxygen atmospheric plasmas is caused by oxygen grafting, i.e. by surface oxidation [13–17]. However, the reality of service life means that when they need to be repaired, composite parts are no longer in a new post-manufacturing state. These parts have experienced an environmental ageing process, including heat, humidity, rain, etc. It can change their chemical structure. Consequences of hygrothermal ageing have been massively studied in the literature: absorption of solvents, migration of additives, plasticization, hydrolysis, oxidation, differential swelling, depolymerization, embrittlement, cracking, etc [18–23].

These changes are problematic for achieving good bonding. Few studies have observed the consequences of pre-bond ageing substrates on the interfacial bonding behaviour. It appears in these studies that there is a decrease in the strength of the bonding joints performed by single lap joint shear test and double cantilever beam test [24–28]. However, there is limited study of the influence of this pre-bond ageing on a bonding protocol that involves surface treatments. The physico-chemical modifications induced on the substrate surfaces were not studied. This paper aims to study the atmospheric plasma contributions on aged composite material surfaces with a bonded repair perspective. This work proposes to observe and analyse their surface modifications on the composite material. To begin, the chemical composition of the material

in its initial state is established. In order to study the aged surfaces, a hygrothermal ageing analysis is necessary. Differences in surface conditions are possible. Atmospheric plasma treatment is then used on unaged and aged surfaces in order to improve bonding. Four types of 3D woven composite material are studied: unaged untreated, unaged treated, aged untreated and aged treated. "Unaged, untreated" refers to an as-received sample, i.e. pristine without plasma treatment. It has been degreased with ethanol. "Unaged, treated" is a pristine sample that has been treated with atmospheric plasma. "Aged, untreated" is a sample aged in immersion at 70°C, which has not received any surface treatment. It has just been degreased with ethanol. Finally, "Aged, treated" is a 70°C immersion-aged sample that has received atmospheric plasma treatment.

The objective is to compare their morphology, roughness, and surface chemistry. Alterations of ageing, thus positive and negative effects of plasma on the materials are coupled.

## 2. Material and methods

### 2.1. Material

The composite material used in this study is a 3D woven fabric. Carbon fibres are used as reinforcement, while an aeronautical epoxy/amine is used as matrix. Silicon and calcium-based particles are present in the material. The epoxy resin formulation, the 3D woven fabric architecture and the particle nature are confidential. The initial glass transition temperature is  $T_g=151.6 \pm 1.2$  °C (obtained by TA Instruments DSC Q200, temperature at midpoint). The samples have the following dimensions:  $50 \times 50 \times 9.5$  mm<sup>3</sup>.

#### 2.1.1. Hygrothermal ageing

Hygrothermal ageing of samples has been carried out in immersion in distilled water at 70 °C in a Climats VRT Extreme 320 climatic chamber during 450 days. They were periodically removed from the water and weighted using a 0.1 mg resolution Mettler AE 200 electronic balance. Before hygrothermal ageing, the samples are stocked in an air-conditioned room ( $20 \pm 1$  °C,  $35 \pm 5$  %RH).

#### 2.1.2. Plasma treatment

The samples are degreased with ethanol before atmospheric plasma treatment. A FG5001+RD1004 OpenAir Plasmastreat atmospheric pressure plasma system is used. The nozzle projects dry compressed air with a pressure of 1-1.5 bar. It is struck with radio frequency (RF) power at 15-25 MHz. The generator power is 1 kW. A PT60 OpenAir Plasmastreat table is used to precisely translate the plasma source along the sample's length. The plasma parameters are the translation speed of the nozzle, the distance between the nozzle and the sample surface and the numbers of scans on the surface sample. Plasma treatment optimization is reached as a minimal contact angle between a drop of distilled water and the sample, hence

the higher value of surface free energy of the composite is obtained. The optimized parameters are a distance of 10 mm, a nozzle speed of 1m/min and three scans.

## 2.2. Methods and instrumentation

### 2.2.1. Scanning electron microscopy (SEM)

Before and after atmospheric plasma treatment, the surface morphology of the unaged and aged samples is observed using the ZEISS EVO HD15 environmental scanning electron microscope (SEM). As samples surfaces are not metallized, observations were made in a degraded vacuum with a pressure of 20 Pa. Pictures were performed with backscattered electron radiation. This type of electron is sensitive to the atomic number of the atoms constituting the sample. Heavier atoms will re-emit more electrons than lighter atoms and appear brighter. These measurements are complemented by AZtec energy-dispersive spectroscopy (EDS) from Oxford Instruments to verify the chemical composition of the sample surface. EDS maps are used to analyse chemical composition and distribution. On the maps, white pixels indicate the presence of the chemical element. The more pixels, the more atoms are present. Each SEM and EDS analysis is performed in several areas of the studied samples to confirm the repeatability of the observations.

### 2.2.2. Fourier transform infrared spectroscopy (FTIR)

Fourier transform infrared spectroscopy is used to obtain information on the chemical bonds of functional groups present on the surface of samples. The bonds vibrate at a given frequency, which depends on the atoms and the environment of the bond. Measurements were performed in absorbance on the Perkin-Elmer Spectrum One apparatus with the attenuated total reflectance (ATR) module. The detector type is a mid-infrared toroidal grating spectrograph (MIR TGS) with a wavenumber range of 4000-650  $\text{cm}^{-1}$ . Crystal is a Diamond/ZnSe. After a background, eight scans were performed with a resolution of 1  $\text{cm}^{-1}$ . Corrections of the wavenumber thickness dependence and the baseline were made. The spectra are normalized to the 1510  $\text{cm}^{-1}$  peak, corresponding to the aromatic C=C band, unaffected by ageing [29–31]. Each FTIR spectrum is performed three times per sample to ensure repeatability.

### 2.2.3. Surface roughness

Surface roughness of the untreated and plasma-modified, unaged and aged samples was measured using the Keyence VHX-6000 3D digital microscope and processed using the 3D surface measurement software Vision64 Map. Different parameters are studied to compare the profiles, according to the standard *EN ISO 4287: Geometrical Product Specifications (GPS) — Surface texture: Profile method*.  $R_a$  is the arithmetic average value of filtered roughness and  $R_q$  is the root mean square deviation.  $R_q$ , through its formula, highlights the presence of high peaks or deep valleys. Their formulas are noted below:

$$R_a = \frac{1}{l} \int_0^l |Z(x)| dx \quad (1)$$

$$R_q = \frac{1}{l} \int_0^l |Z(x)|^2 dx \quad (2)$$

Where  $Z(x)$  is the height of the profile for a position on the sample surface  $x$ ,  $l$  is the sampling length. Two other parameters are used and defined below:  $R_{sk}$  the profile skewness and  $R_{ku}$  the kurtosis that means the flattening coefficient of the profile.

$$R_{sk} = \frac{1}{R_q^3} \left[ \frac{1}{l} \int_0^l Z(x)^3 dx \right] \quad (3)$$

$$R_{ku} = \frac{1}{R_q^4} \left[ \frac{1}{l} \int_0^l Z(x)^4 dx \right] \quad (4)$$

$R_v$  and  $R_p$  are respectively the maximum depth of the valleys and the maximum height of the peaks.

#### 2.2.4. X-ray photoelectron spectroscopy (XPS)

X-ray photoelectron spectroscopy analysis was carried out to determine the functional groups and their content on the surface of the untreated and plasma-modified, unaged and aged specimens. Thermo K-alpha+ X-ray photoelectron spectroscope with the monochromatic Al K $\alpha$  X-ray radiation was used. The analysed depth is approximately 3 nm. Pass energies of 19 eV (0.1 eV step) were used for the high-resolution spectra. Ten scans for each high-resolution spectrum of the XPS main  $C_{1s}$  peaks were recorded. No neutralization was needed for the samples. The calibration was done with the main component of the  $C_{1s}$  peak, associated with the value of 284.7 eV [32, 33]. The  $C_{1s}$  spectra of all samples were fitted using the PHI-MATLAB data-processing software. All spectra are referenced to the  $C_{1s}$  peak for neutral carbon.

### 3. Results

#### 3.1. Unaged samples state

A study on the unaged samples before and after plasma treatment was carried out. Morphology, and chemical composition and distribution are analysed by SEM and EDS in Figures 1 and 2. The SEM images are associated with EDS maps showing the main chemical elements present in the sample. The darker areas correspond to the carbon fibres, while the lighter areas are associated with the epoxy-amine matrix. Particles appear brighter on backscattered electrons SEM images of the surface view because the atoms constituting them are heavier than those composing the matrix and the fibres. Carbon and oxygen atoms are associated with the resin. The carbon also corresponds to the fibres. The chlorine atoms are part of the composition of the amine incorporated in the matrix. Other chemical elements are also regularly distributed in the unaged material: silicon and calcium. They are also present in the composite bulk and the neat resin bulk.

FTIR analysis in Figure 3 allows the identification of the matrix different absorption bands before their chemical evolution. The spectra are identical for the neat resin and the composite material. The band from

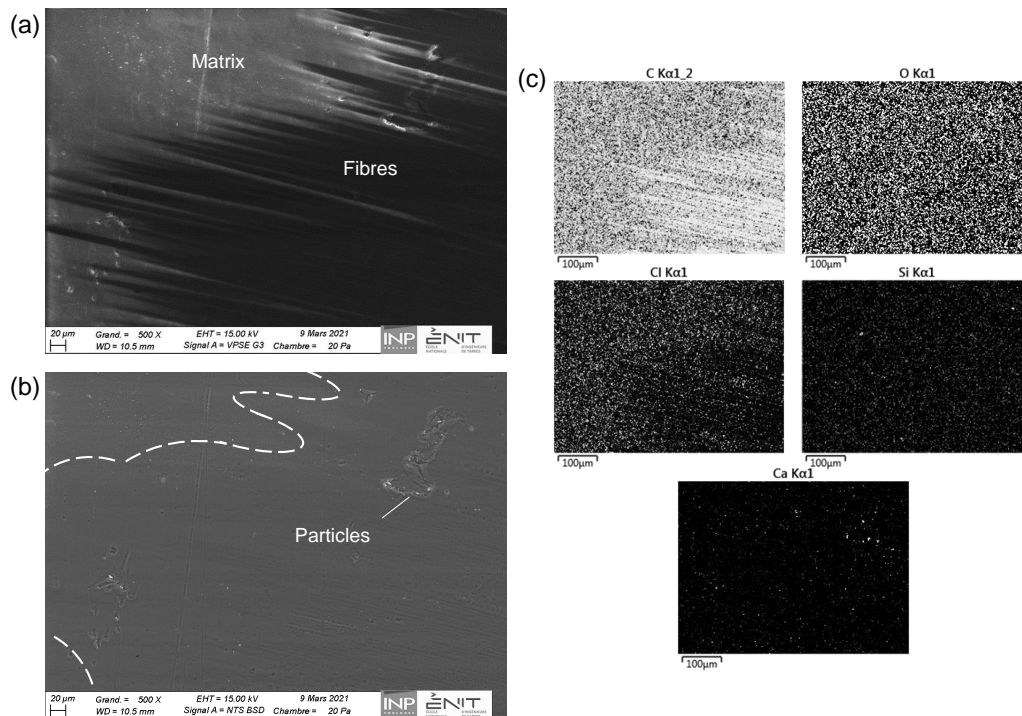


Figure 1: Surface view of the unaged composite material (a) secondary electron SEM picture, (b) backscattered electron SEM picture, (c) EDS maps of principal chemical elements.

3650 to 3150  $\text{cm}^{-1}$  corresponds to O-H bonds. The double peak at 3050  $\text{cm}^{-1}$  is associated with primary amine N-H bond elongations. The double peak at 2850  $\text{cm}^{-1}$  is linked to alkane C-H bond and secondary amine N-H elongation. At 1730  $\text{cm}^{-1}$ , the peak is assigned to the C=O bond. The peaks at 1600, 1510, and 1455  $\text{cm}^{-1}$  represent aromatic C=C bonds. The various peaks from 1225 to 1025  $\text{cm}^{-1}$  are related to the amine C-N, and aromatic C-H bonds [31, 34–36]. At 1025  $\text{cm}^{-1}$ , a Si-O peak may be identified due to the presence of silicon identified by EDS. Some authors have already observed this peak on silica [37–40] or E-glass [41, 42]. This Si-O peak is due to the presence of silicon and calcium-based particles in the samples whose chemical composition in unaged composite and neat resin samples had been identified by EDS. Silica spectra, characterized by the Si-O peak at 1025  $\text{cm}^{-1}$ , is presented in Figure 3. This preliminary analysis provides an indication of the initial chemical composition of the materials used.

### 3.2. Effects of hygrothermal ageing

Figure 4 shows the sorption curves obtained by gravimetry in immersion at 70 °C for woven 3D composite materials with dimensions of  $50 \times 50 \times 9.5 \text{ mm}^3$ , but also for neat resin with dimensions of  $10 \times 10 \times 3 \text{ mm}^3$ . Carbon fibres being impermeable, the composite mass variations in percentage are reduced to the matrix mass fraction. To overcome thickness shifts, the square root of time in seconds is divided by the thickness in millimetres. After 450 days of ageing, saturation is not reached. Mass uptake of neat resin and composite

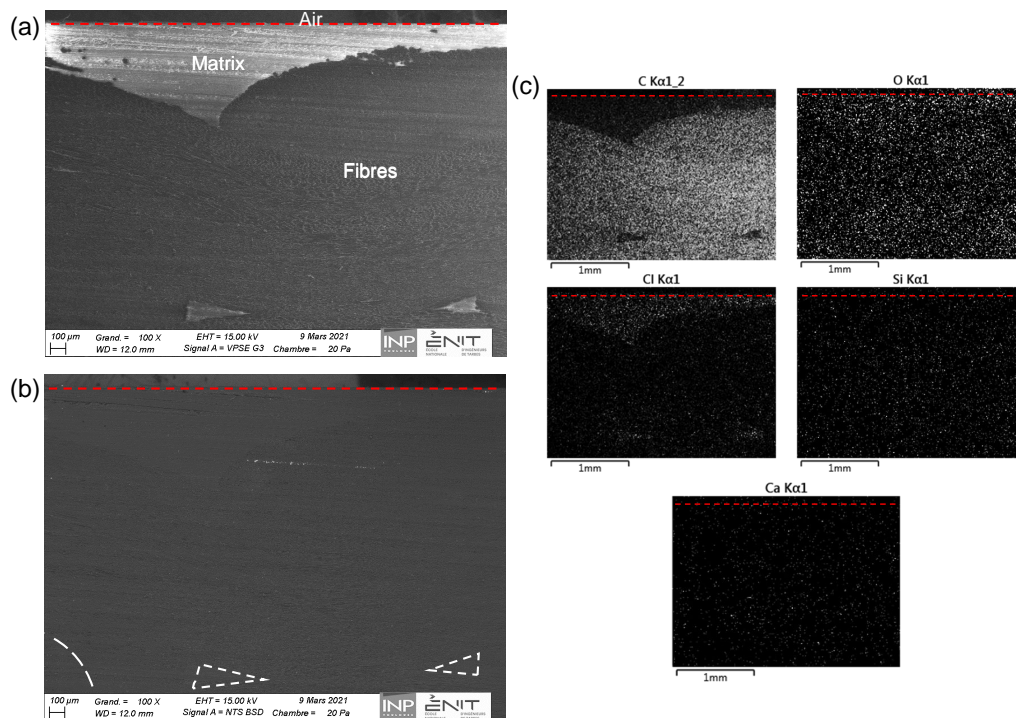


Figure 2: Slide view of the unaged composite material (a) secondary electron SEM picture, (b) backscattered electron SEM picture, (c) chemical element EDS maps of principal chemical elements. Image depth: 2 mm.

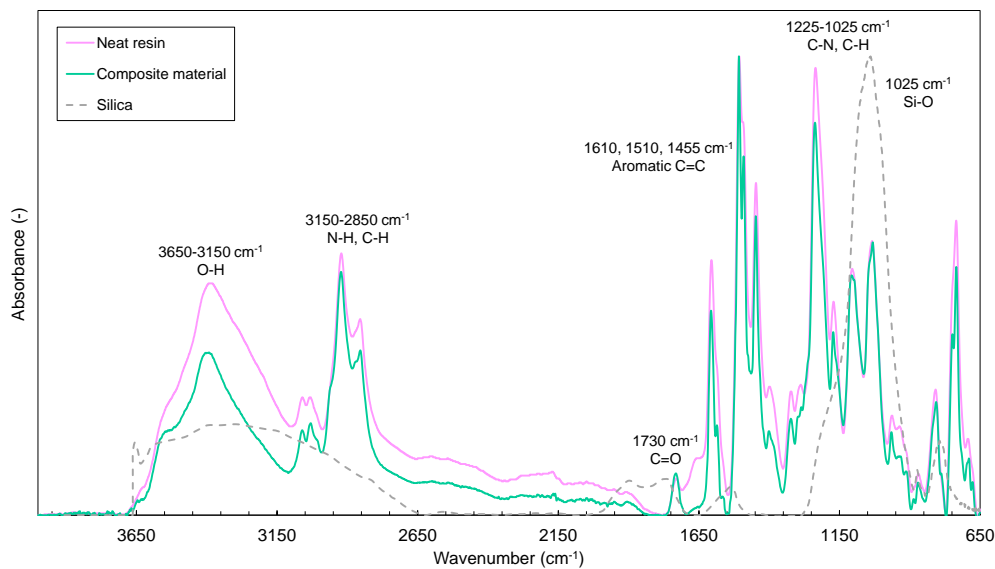


Figure 3: FTIR spectra of unaged neat resins, composite materials and silica.

matrix are respectively  $1.21 \pm 0.02$  % and  $1.07 \pm 0.003$  %. In the neat resin, the water absorption has slowed down after a first diffusion step reached after about 16 days of sorption. It has led to a second diffusion

stage. In contrast, the water diffusion in the composite’s matrix does not reach a second diffusion stage yet. It still seems to be on the first diffusion stage but could eventually achieve a higher water mass uptake. Despite this ratio, the diffusion kinetics of the composite’s matrix differs from that of the neat resin, which may suggest that the presence of the fibres has modified this kinetics.

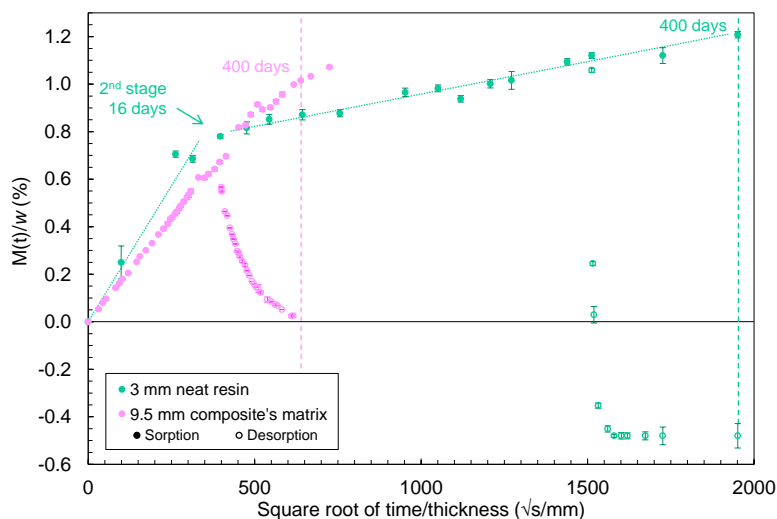


Figure 4: Water sorption curves in immersion at 70 °C followed by water desorption curve in an oven at 70 °C, reduced to the matrix mass fraction.

During the hygrothermal ageing, some samples are placed in an oven at 70 °C to be desorbed. After about 30 days of desorption, the neat resin curve reaches the equilibrium stage. The desorbed samples do not regain their initial mass but fall to a lower value of  $-0.48 \pm 0.06$  %. After more than 200 days of desorption, the composite samples have not yet reached an equilibrium stage and the desorption, although slowed, continues. With a negative mass uptake after desorption, the neat resin curve highlights irreversible mass losses. Therefore, several reversible and irreversible phenomena take place simultaneously and may be opposed during the moisture absorption phase. Indeed, an apparition of white particles is noticeable in the water of the immersion beakers. These may be due to extraction from the neat resin and composite samples. It results in mass losses that distort the gravimetric measurements by lessening the mass uptake.

Results in FTIR of materials at different ageing times and these white particles are shown in Figure 5. Spectra of extracted particles are characterized by the large peak at  $1090-890$   $\text{cm}^{-1}$  corresponding to Si–O bonds. The band from  $3650$  to  $3050$   $\text{cm}^{-1}$  is associated with O–H and Si–O–H bonds, while the peak at  $3600$   $\text{cm}^{-1}$  is assigned to isolated silanol vibrations. These bands are linked to the infrared spectra of silica [37, 40]. They are also found in the spectra of aged material surfaces.  $1090$  and  $1025$   $\text{cm}^{-1}$  peaks present on unaged spectra merge and intensify with ageing time. Particles may have moved and been deposited to the surface due to ageing. Moreover, other chemical alterations are noticeable. The band from  $3750$  to  $3150$

$\text{cm}^{-1}$  linked to O–H bonds is marked by a strong increase caused by the absorption of water molecules. The disappearance of the peaks at  $3050 \text{ cm}^{-1}$  and  $2850 \text{ cm}^{-1}$  is observed and can be related to the hydrolysis of N–H and C–H bonds [43]. Finally, a peak appears at  $1650 \text{ cm}^{-1}$ . It may correspond to oxygen grafting leading to the formation of C=O bonds [44, 45]. Spectra of the pure resin and the composite material show the same alterations after ageing.

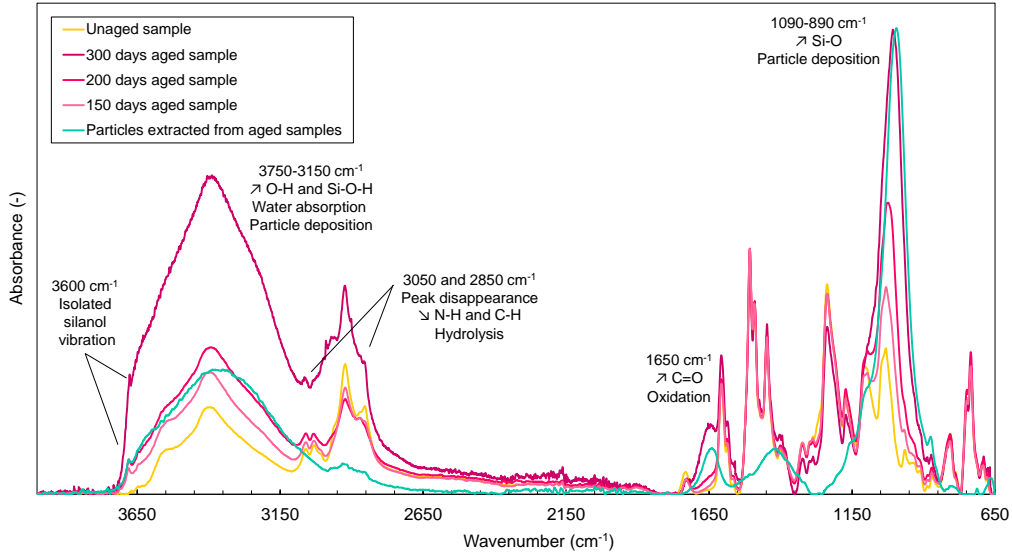


Figure 5: FTIR spectra of composite materials at different ageing times (unaged, 150, 200 and 300 days) and of extracted particles.

SEM microscopies are performed with backscattered electron radiation on aged neat resins and composite materials. Figures 6 and 7 highlight the particles. They appear white on the SEM pictures. The hydrothermal ageing process causes agglomeration of particles on the surface of the neat resin and the composite material. In addition, cracks and crevices are also visible. They can be linked, on the one hand, to leaching of the material due to hydrolysis, and on the other hand, to a migration and deposition of the particles. Abdessalem noted this migration of particles during ageing and highlighted the effect of osmotic pressure [46]. Under the action of water, the additives rise to the surface and agglomerate. The resin also appears lighter in colour on Figures 6 and 7, probably as a result of particle clustering and deposition.

### 3.3. Effects of plasma treatment on aged samples

#### 3.3.1. Roughness measurements

Sample profiles measurements are presented in Table 1. In the state of reception (unaged, untreated samples), roughness values of  $R_a = 10.20 \pm 0.26 \mu\text{m}$  and  $R_q = 12.88 \pm 0.22 \mu\text{m}$  are reported. Its skewness  $R_{sk}$  is less than 0. According to *EN ISO 4287* standard, the profile shows more peaks, clipped, than valleys.

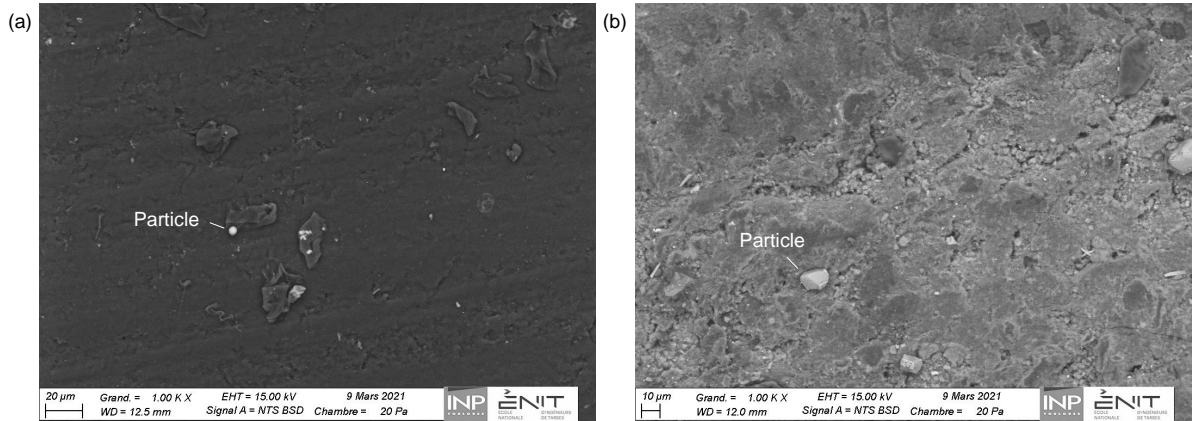


Figure 6: SEM pictures of neat resin (a) unaged untreated, (b) aged untreated (400 days) Backscattered electron images.

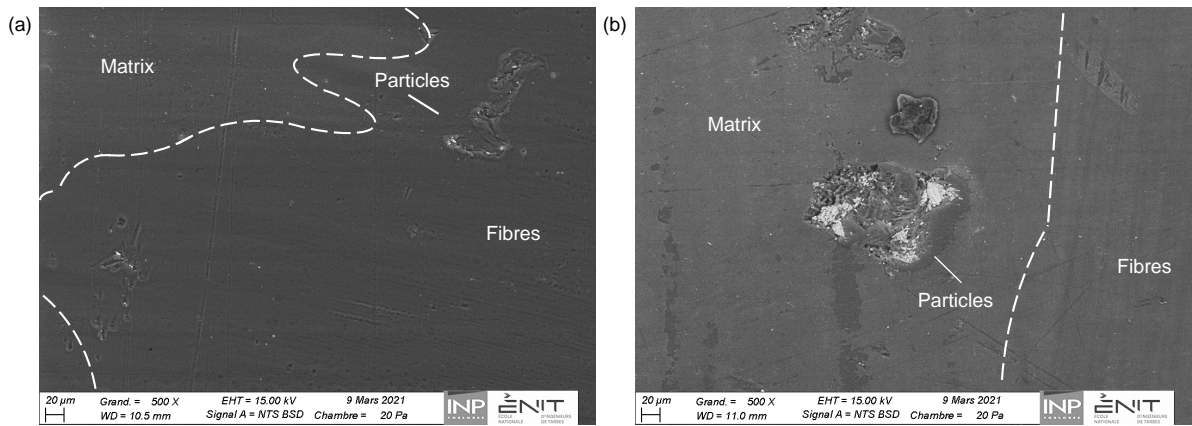


Figure 7: SEM pictures of composite material (a) unaged untreated, (b) aged untreated (400 days). Backscattered electron images.

Kurtosis  $R_{ku}$  is greater than 3; the profile has very tight peaks or valleys, which is also found with the maximum heights and depths  $R_p = 50.26 \pm 7.36 \mu\text{m}$  and  $R_v = -74.34 \pm 13.17 \mu\text{m}$ .

Plasma treatment slightly reduces the roughness  $R_a$  and  $R_q$  of the samples. The difference between the zero level and the maximum depths  $R_v$  is smaller than untreated samples, suggesting material erosion. With respect to the uncertainties,  $R_p$  does not vary considerably. Furthermore, SEM microscopies highlight larger or agglomerated particles, which appear brighter in backscattered electrons. EDS cartographies reveal silicon clusters and calcium increase in Figure 8. Plasma treatment will etch the polymer matrix at a faster rate than silicon-based particles. Therefore, more particles will be agglomerated on the surface after plasma treatment. These particle clusters may result in no decrease in  $R_p$ .

During ageing, a deposit seems to be created during immersion. It could be caused by extraction of material, such as particles present in the sample, highlighted by SEM and EDS in the Figure 9. After 400 days of ageing, the silicon and calcium compositions on the surface rise uniformly. It is possible to observe

Table 1: Roughness parameters of unaged and aged (400 days), untreated and treated samples: Arithmetic average roughness  $R_a$ , root mean square roughness  $R_q$ , skewness parameter  $R_{sk}$ , kurtosis parameter  $R_{ku}$ , maximum peak  $R_p$ , maximum valley  $R_v$  and maximum peak to valley  $R_z$ .

	Unaged, untreated	Unaged, treated	Aged, untreated	Aged, treated
$R_a$ ( $\mu\text{m}$ )	$10.20 \pm 0.26$	$9.07 \pm 0.64$	$9.84 \pm 0.06$	$8.33 \pm 1.59$
$R_q$ ( $\mu\text{m}$ )	$12.88 \pm 0.22$	$10.98 \pm 0.78$	$12.39 \pm 0.06$	$11.04 \pm 1.93$
$R_{sk}$	$-0.37 \pm 0.24$	$-0.36 \pm 0.39$	$-0.26 \pm 0.17$	$0.025 \pm 0.75$
$R_{ku}$	$3.45 \pm 0.36$	$3.09 \pm 0.11$	$3.24 \pm 0.04$	$4.00 \pm 0.36$
$R_p$ ( $\mu\text{m}$ )	$50.26 \pm 7.36$	$51.47 \pm 10.32$	$57.53 \pm 9.10$	$61.31 \pm 25.69$
$R_v$ ( $\mu\text{m}$ )	$-74.34 \pm 13.17$	$-55.52 \pm 4.44$	$-64.53 \pm 6.75$	$-55.74 \pm 5.14$
$R_z$ ( $\mu\text{m}$ )	$124.60 \pm 20.54$	$106.98 \pm 14.76$	$122.06 \pm 15.84$	$117.04 \pm 30.82$

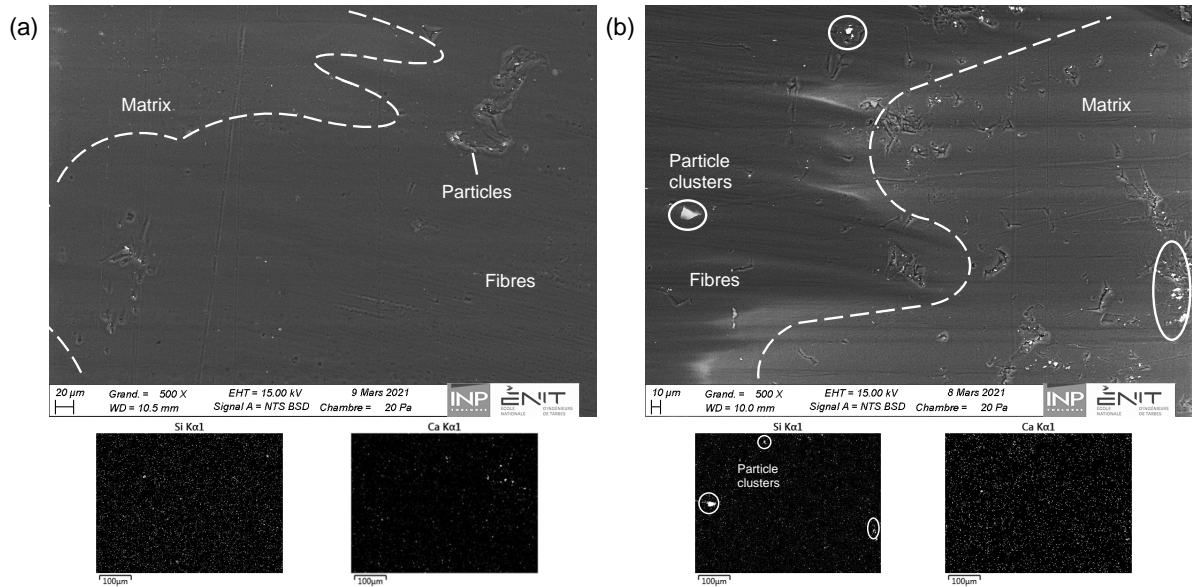


Figure 8: SEM picture with EDS maps of unaged composite material (a) unaged untreated, (b) unaged treated. Backscattered electron images.

this on the EDS maps where the presence of silicon has strongly increased compared to the unaged samples maps (Figure 8).  $R_a$  and  $R_q$  are very slightly reduced. An increase in the height of peaks  $R_p$  and a reduction in the depth of valleys  $R_v$  are observed (Table 1). They may be caused by the migration and deposition of the particles on peaks and valleys.

Concerning the aged treated samples, the roughness parameters  $R_a$  and  $R_q$  are reduced enough compared to unaged untreated samples. The valleys  $R_v$  are shallower. The variability of the  $R_p$  value is very high

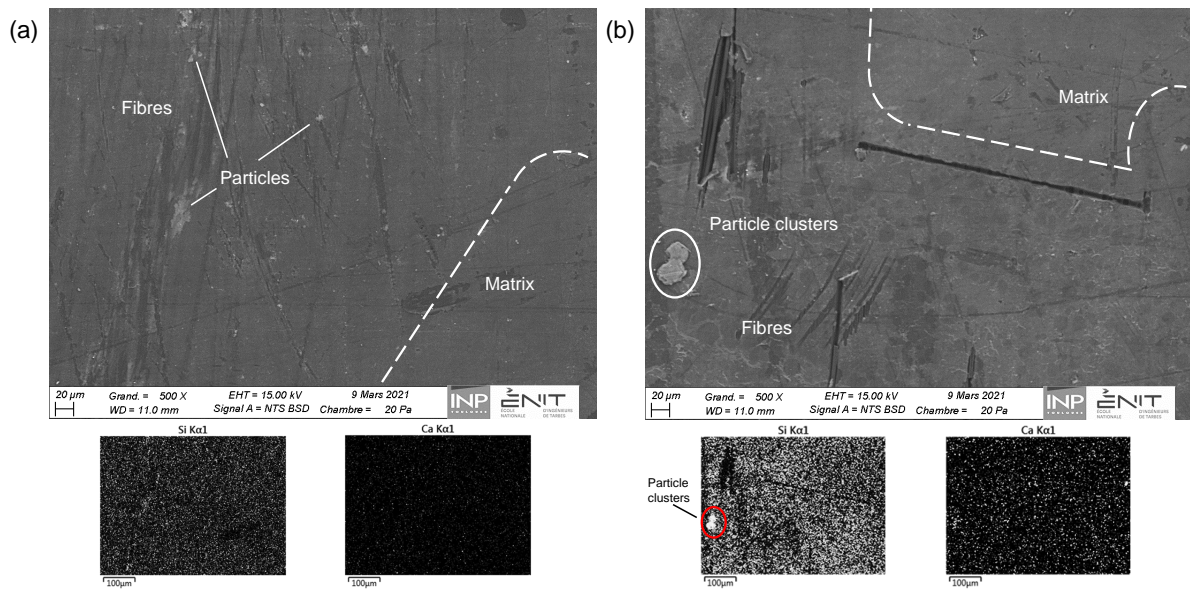


Figure 9: SEM picture with EDS maps of 400-days aged composite material (a) aged untreated, (b) aged treated. Backscattered electron images.

and does not confirm its increase. However, this high standard deviation reflects a significant irregularity of the aged treated surface. While the epoxy resin seems sensitive to the plasma's heat, the silicon-based particles withstand much higher temperatures. By EDS, particle deposition related to ageing and particle agglomeration linked to plasma-induced matrix degradation (circled spot) are visible (Figure 9). Particle deposition due to ageing, matrix erosion and particle cluster formation due to plasma could explain this significant irregularity in the highest peak values  $R_p$ . For the four specimen types, the parameter  $R_{ku}$  is always respectively higher than 3. Despite treatment and conditioning, the valleys and peaks remain tight. While the unaged untreated, unaged treated and aged untreated samples all show a negative  $R_{sk}$ , it is greater than 0 for the aged treated ones. However, a significant standard deviation is noticeable, suggesting that the surfaces are pretty irregular. Some areas are probably more provided with particles that will decrease the plasma heat's action and thus impact the size and shape of the peaks. Therefore, the silicon particles extraction during ageing seems to increase the maximum heights and decrease the maximum depths by covering the surface. In contrast, the plasma treatment reduces maximum heights and depths by eroding the surface.

### 3.3.2. Surface chemistry

To obtain information on the surface chemistry, X-ray photoelectron spectroscopy (XPS) measurements are carried out. Table 2 gives the relative proportions of the different chemical elements. 7 chemical elements are identified: oxygen, nitrogen, carbon, chlorine, silicon and calcium. Table 3 gives some of their ratios: O/C, N/C, Si/C and Cl/C. Figure 10 regroups the high resolution  $C_{1s}$  spectra for each case and allows the

identification of the chemical groups related to carbon. The  $C_{1s}$  peak of unaged untreated samples is fitted with 5 components:  $\underline{C}=\underline{C}$  and  $\underline{C}-\underline{Si}$ ,  $\underline{C}-\underline{C}$ ,  $\underline{C}-\underline{O}$  and  $\underline{C}-\underline{N}$ ,  $\underline{C}-\underline{Cl}$ ,  $\underline{COO}-\underline{C}$  and  $\underline{CON}-\underline{C}$ . Table 4 gives the proportions of some functional groups of  $C_{1s}$  and  $O_{1s}$  spectra.

Table 2: Element composition (%) according to the plasma treatment and ageing (250 days), performed by XPS.

Element	$O_{1s}$	$N_{1s}$	$Ca_{2p}$	$C_{1s}$	$Cl_{2p}$	$Si_{2s}$	$Si_{2p}$
Position (eV)	533	400	348	285	201	169	103
Unaged untreated	$18.2 \pm 0.9$	$4.3 \pm 0.2$	$0.45 \pm 0.02$	$68.9 \pm 3.9$	$0.91 \pm 0.05$	$1.0 \pm 0.05$	$5.9 \pm 0.3$
Unaged treated	$29.4 \pm 1.5$	$2.9 \pm 0.1$	$0.50 \pm 0.02$	$55.3 \pm 2.8$	$0.65 \pm 0.03$	$1.4 \pm 0.05$	$9.5 \pm 0.5$
Aged untreated	$26.2 \pm 1.3$	$2.1 \pm 0.1$	$2.20 \pm 0.11$	$58.2 \pm 2.90$	$0.11 \pm 0.01$	$1.47 \pm 0.07$	$8.98 \pm 0.04$
Aged treated	$23.9 \pm 1.2$	$1.30 \pm 0.06$	$4.9 \pm 0.2$	$41.2 \pm 2.0$	$0.10 \pm 0.05$	$1.47 \pm 0.07$	$23.2 \pm 1.2$

Table 3: Chemical elements ratios according to plasma treatment and ageing (250 days), performed by XPS.

Ratio	O/C	N/C	Si/C	Cl/C
Unaged untreated	0.26	0.06	0.10	0.013
Unaged treated	0.53	0.05	0.19	0.011
Aged untreated	0.45	0.04	0.18	0.002
Aged treated	0.58	0.03	0.60	0.002

Plasma causes strong surface oxidation [14, 47], illustrated by the increase in the O/C ratio and the proportions of  $-(\underline{C}=\underline{O})-\underline{O}$  bonds, as well as the decrease in the bonds:  $\underline{C}-\underline{OH}$ ,  $\underline{C}-\underline{O}-\underline{C}$ ,  $-(\underline{C}=\underline{O})-\underline{O}$ ,  $-(\underline{C}=\underline{O})-\underline{N}$  and  $\underline{Si}-\underline{O}-\underline{Si}$  [48]. Surface degradation of the matrix and fibres is also suspected. Indeed, the proportions of carbon, nitrogen and chlorine decrease while those of oxygen and silicon increase. In addition, satellite shake-up  $\pi - \pi^*$  band appears on the high-resolution spectrum  $C_{1s}$  after processing. Representative of the aromatic and graphitic structures, it is not or hardly detectable on epoxy resins. The shake-up  $\pi - \pi^*$  band appearance implies the exposure of carbon fibres [49, 50]. The proportion of  $C_{sp2}$  is as well accentuated with treatment. These different variations confirm plasma-induced erosion of the epoxy matrix.

Various phenomena illustrate the ageing of samples. Moisture absorption can be observed by the decrease of  $\underline{C}-\underline{C}$  bonds and the increase of  $\underline{C}-\underline{O}$  [51]. These variations could also be due to oxidation, mainly in the form of hydroxyl or ether. Although weaker than with plasma treatment, oxidation is noticeable, illustrated by the increase in the O/C ratio. As previously, the shake-up band  $\pi - \pi^*$  appears, a sign of the exposure of the carbon fibres. The decrease in the N/C and Cl/C ratios is noticeable, reflecting a disappearance of the

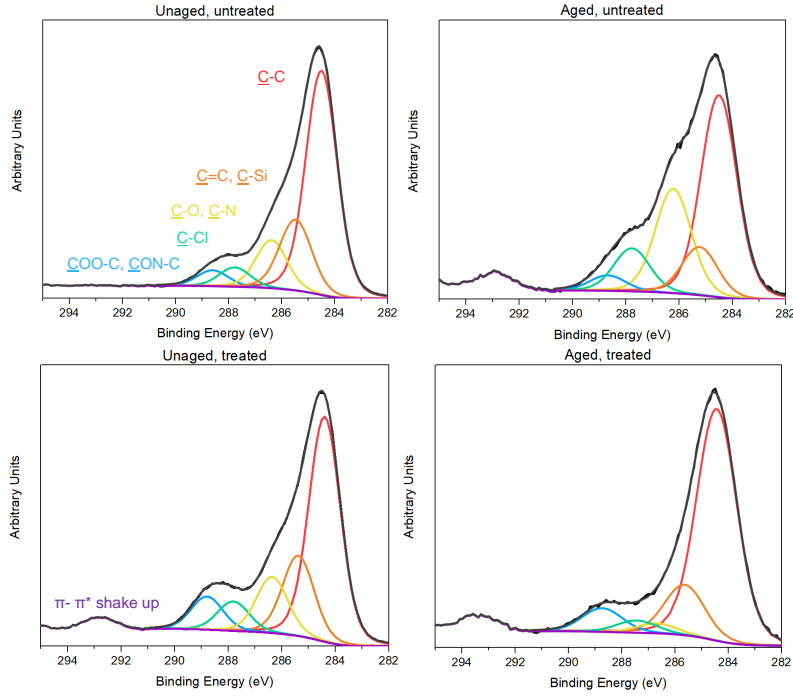


Figure 10: XPS spectra of  $C_{1s}$  according to plasma treatment and ageing (250 days).

Table 4: Functional groups proportions for  $C_{1s}$  and  $O_{1s}$  (%) according to plasma treatment and ageing (250 days), performed by XPS.

Functional group	$\underline{C=C}$ , $\underline{C-Si}$ ( $C_{1s}$ )	$\underline{C-C}$ ( $C_{1s}$ )	$\underline{C-O}$ , $\underline{C-N}$ ( $C_{1s}$ )	$\underline{C-Cl}$ ( $C_{1s}$ )	$\underline{COO-C}$ , $\underline{CON-C}$ ( $C_{1s}$ )	$-(\underline{C=O})-O$ , $C-\underline{O}-C$ , $C-\underline{O}H$ , $-(\underline{C=O})-N$ , $Si-\underline{O}-Si$ ( $O_{1s}$ )	$-(\underline{C=O})-\underline{O}$ ( $O_{1s}$ )	$-(\underline{C=O})-\underline{O}$ ( $C=O$ ), $\underline{O}-(\underline{C=O})$ $-O$ ( $O_{1s}$ )
Position (eV)	284.5	285.4	286.4	287.7	288.7	532.4	533.4	534.0
Unaged untreated	58.9	19.2	12.6	5.1	4.2	72.4	27.6	-
Unaged treated	53.0	19.0	25.3	7.0	3.7	21.7	68.4	9.9
Aged untreated	48.9	11.7	13.2	10.4	7.8	58.2	41.8	-
Aged treated	70.7	15.4	3.0	3.7	7.2	64.9	35.1	-

epoxy-curing bonds ( $-\text{COH}-\text{CH}_x-\text{NH}-$ ), which could be caused by hydrolysis [51]. These different variations suggest leaching of the matrix during ageing. The various chemical degradations observed irreversibly alter the resin, which can embrittle the surface of the samples and reduce their mechanical properties.

In addition, a strong increase in the silicon and Si/C ratio is observed after moisture absorption especially when followed by plasma treatment, which seems to be related to the extraction of the silicon particles. Plasma treatment on aged samples leads to the following observations. The  $\text{C-O}$  and  $\text{C-N}$  bonds which had increased with the presence of water decreased strongly with the plasma which induces a desorbing effect of the plasma. Finally, according to the O/C ratios, the oxidation induced is similar to that of an unaged treated sample.

#### 4. Discussion

Figure 11 illustrates the 4 types of samples studied in this paper.

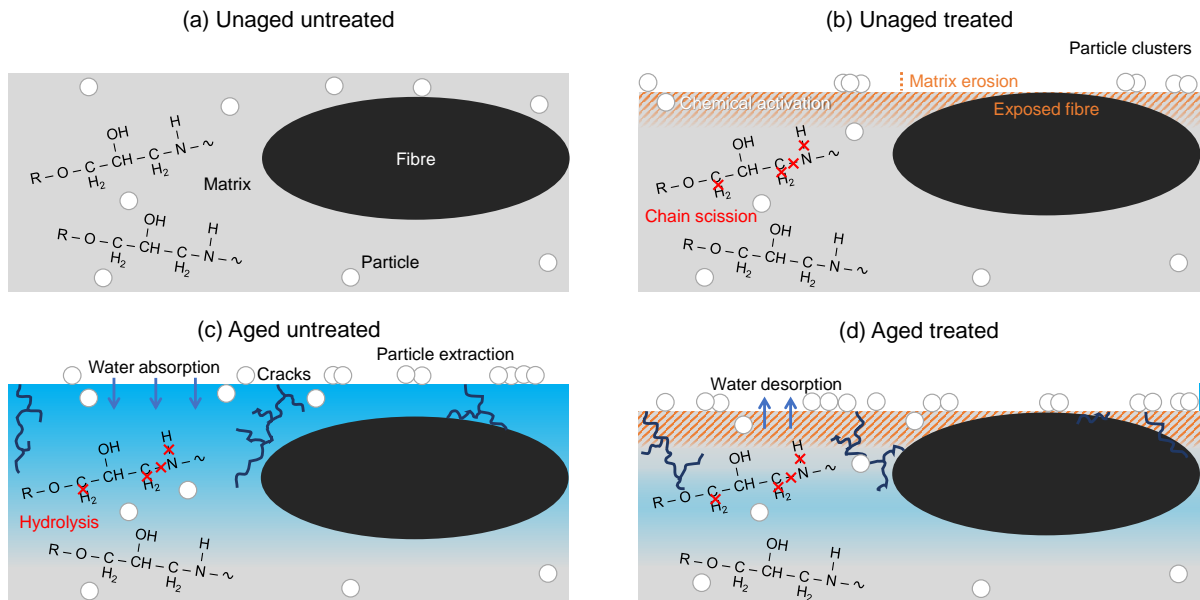


Figure 11: Ageing and plasma induce phenomena schematisation.

In the unaged untreated state, the 3D woven composite material samples are constituted of an epoxy-amine matrix reinforced with carbon fibres. Small particles composed of silicon and calcium are observable by SEM, EDS and XPS (Figure 11 (a)).

During the study, some unaged samples were treated with plasma (Figure 11 (b)). Effects of atmospheric plasma treatment on unaged surfaces are known: oxidation by oxygen grafting, surface free energy increase by polarization, higher wettability, slight topological changes. Some chain scission due to the thermal action of the plasma are nevertheless observed as it happened in other papers [14, 16, 52–56].

Concerning aged samples (Figure 11 (c)), water absorption causes oxidation and hydrolysis of the matrix, which leads to some scissions of the epoxy/hardener chains and microcracks, as observed in other studies [21, 22, 45, 57]. This water absorption is counterbalanced by mass losses observed in desorption during

gravimetry. These mass losses are linked to hydrolysis but also particles extraction and deposition in the surface [46, 58–61]. These phenomena are confirmed in different analyses. SEM coupled with EDS allows observing a modification of the surfaces, including cracks on the aged neat resin and an increase of silicon and calcium atom numbers. XPS analyses demonstrate the oxygen and silicon percentages increase, highlighting, on the one hand, oxidation and moisture absorption and, on the other hand, migration of particles to the surface. Comparing the plasma treated specimens, the same oxidation phenomena are observed by XPS whether the specimens are unaged or aged. The decrease of bonds associated with the amine percentage shows hydrolysis of this one as reported in the literature [51]. The FTIR analyses show the appearance of peaks associated with silicon particles and water molecules absorption on the surface and bands linked to amine bonds attenuation.

Different actions of atmospheric plasma on hygrothermal aged samples are reported (Figure 11 (d)). Using plasma treatment on aged samples, irreversible ageing effects remain, such as the breaking down of epoxy/hardener bonds by hydrolysis and particles extraction and accumulation on the surface, which may embrittle the surface matrix. Nevertheless, XPS has revealed a desorbing effect in surface compared to aged untreated samples. Although having a slightly degrading thermal action, atmospheric plasma on aged samples allows the recovery of dry surfaces before in-situ bonded repair. Comparing the surface topologies makes it possible to see that aged treated samples have similar  $R_p$  values to aged untreated ones and similar  $R_v$  values to unaged treated specimens. A substantial variability is still observed. It is due to the particles rise and carbon fibre exposure, increasing the size of the peaks and to the thermal erosion of the matrix by plasma, decreasing the differences between maximum and minimum peaks size.

## 5. Conclusion

This paper aims to analyse atmospheric plasma surface contributions for a bonded repair on carbon/epoxy 3D woven composite materials that are no longer in their initial state. The surfaces chemical evolution following hygrothermal ageing was analysed. It shows different phenomena: water absorption on the surface, hydrolysis, bond breaks, oxidation, migration of particles, which can impact the surface adhesion. The visible results of these alterations are cracks and a deposit of particles on the surface. Atmospheric plasma treatment allows, despite slight thermal degradation, to chemically activate unaged and aged surfaces by oxygen grafting. Desorption is found on the aged treated surfaces because of the thermal action of plasma.

Therefore, the surface to be treated and repaired can be dry, even though the rest of the sample may have absorbed water and thus aged. Nevertheless, the migration of particles on the surface has caused contamination and irregular topology variations. Considering these findings, repair bond adhesion could be affected. As a result, interfacial strength measured by adherence tests on the four types of 3D woven

composite surfaces coated by an adhesive layer will be analysed related to the multiple phenomena previously exposed.

## 6. Acknowledgment

The authors express their sincere thanks to SAFRAN Aircraft Engines, France, and the Agence Nationale de la Recherche et de la Technologie for the financial support (ANRT CIFRE n°2018/0355 project). They are grateful to Céline Brunon from Science et Surface, France, for performing XPS experiments, Amandine Abadie and Nathalie Aubazac at the Laboratoire Génie de Production, France, for their technical support.

## References

- [1] Lee Henry and Neville Kris. *Handbook of Epoxy Resins*. McGraw-Hill, New York, 1967.
- [2] Stan T. Peters, editor. *Handbook of composites*. Springer Science+Business Media Dordrecht, London, 2nd edition edition, 1998. OCLC: 833259792.
- [3] A. Baker, S. Dutton, and D. Kelly. *Composite materials for aircraft structures*. American Institute of Aeronautics and Astronautics, Inc., 2004.
- [4] A. A. Baker, A. J. Gunnion, and J. Wang. On the certification of bonded repairs to primary composite aircraft components. *The Journal of Adhesion*, 91:4–38, 2015.
- [5] F. Collombet, Y.-H. Grunevald, L. Crouzeix, B. Douchin, R. Zitoune, Y. Davila, A. Cerisier, and R. Thévenin. Repairing composites. In P. Boisse, editor, *Advances in Composites Manufacturing and Process Design*, pages 197–227. Woodhead Publishing, 2015.
- [6] C. H. Wang and A. J. Gunnion. On the design methodology of scarf repairs to composite laminates. *Composites Science and Technology*, 68(1):35–46, 2008.
- [7] J. Cognard. Some recent progress in adhesion technology and science. 9(1):13–24, 2006.
- [8] M. Préau. *Defect Management in Vacuum Bag Only Semipreg Processing of Co-bonded Composite Repairs*. Phd thesis, McGill University, Department of Mechanical Engineering, Montréal, Québec, Canada, 2016.
- [9] Barbora Nečasová, Pavel Liška, Jakub Kelar, and Jiří Šlanhof. Comparison of Adhesive Properties of Polyurethane Adhesive System and Wood-plastic Composites with Different Polymers after Mechanical, Chemical and Physical Surface Treatment. *Polymers*, 11(3):1–17, 2019.
- [10] L. Kumosa, D. Armentrout, and M. Kumosa. The effect of sandblasting on the initiation of stress corrosion cracking in unidirectional E-glass/polymer composites used in high voltage composite non ceramic insulators. *Composites Science and Technology*, 62(15):1999–2015, 2002.
- [11] Sam Siau, Alfons Vervaet, Andre Van Calster, Ives Swennen, and Etienne Schacht. Epoxy polymer surface roughness modeling based on kinetic studies of wet chemical treatments. *Journal of The Electrochemical Society*, 151(8):54–61, 2004.
- [12] K.B. Katnam, L.F.M. Da Silva, and T.M. Young. Bonded repair of composite aircraft structures: A review of scientific challenges and opportunities. *Progress in Aerospace Sciences*, 61:26–42, 2013.
- [13] C. Tendero, C. Tixier, P. Tristant, J. Desmanson, and P. Leprince. Atmospheric pressure plasmas: A review. *Spectrochimica Acta Part B: Atomic Spectroscopy*, 61(1):2–30, 2006.
- [14] H. Luo, G. Xiong, K. Ren, S. R. Raman, Z. Liu, Q.g Li, C. Ma, D. Li, and Y. Wan. Air DBD plasma treatment on three-dimensional braided carbon fiber-reinforced PEEK composites for enhancement of in vitro bioactivity. *Surface and Coatings Technology*, 242:1–7, 2014.

- [15] X. Chen, L. Yao, J. Xue, D. Zhao, Y. Lan, X. Qian, C.X. Wang, and Y. Qiu. Plasma penetration depth and mechanical properties of atmospheric plasma-treated 3D aramid woven composites. *Applied Surface Science*, 255(5):2864–2868, 2008.
- [16] M. Strobel, M.-J. Walzak, J0 M. Hill, A. Lin, E. Karbasheski, and C. S. Lyons. A comparison of gas-phase methods of modifying polymer surfaces. *Journal of Adhesion Science and Technology*, 9(3):365–383, 1995.
- [17] A. Baldan. Adhesively-bonded joints and repairs in metallic alloys, polymers and composite materials: Adhesives, adhesion theories and surface pretreatment. *Journal of Materials Science*, 39:1–49, 2004.
- [18] X. Colin and Jacques Verdu. Humid Ageing of Organic Matrix Composites. In Peter Davies and Yapa D. S. Rajapakse, editors, *Durability of Composites in a Marine Environment*, Solid Mechanics and Its Applications, pages 47–114. Springer Netherlands, 2014.
- [19] Michael J Adamson. Thermal expansion and swelling of cured epoxy resin used in graphite/epoxy composite materials. *Journal of Materials Science*, 15(7):1736–1745, 1980.
- [20] X Colin, J Verdu, and B Rabaud. Stabilizer Thickness Profiles in Polyethylene Pipes Transporting Drinking Water Disinfected by Bleach. *Polymer Engineering and Science*, 51(8):1539–1549, 2011.
- [21] G.Z. Xiao and M.E.R. Shanahan. Swelling of DGEBA/DDA epoxy resin during hygrothermal ageing. *Polymer*, 39(14):3253–3260, 1998.
- [22] A. Tcharkhtchi, P.Y. Bronnec, and J. Verdu. Water absorption characteristics of diglycidylether of butane diol–3,5-diethyl-2,4-diaminotoluene networks. *Polymer*, 41(15):5777–5785, 2000.
- [23] Y.J. Weitsman. Anomalous fluid sorption in polymeric composites and its relation to fluid-induced damage. *Composites Part A: Applied Science and Manufacturing*, 37(4):617–623, 2006.
- [24] BM Parker. The effect of composite prebond moisture on adhesive-bonded CFRP-CFRP joints. *Composites*, 14(3):226–232, 1983.
- [25] D.N. Markatos, K.I Tserpes, E. Rau, S. Markus, B. Ehrhart, and Sp. Pantelakis. The effects of manufacturing-induced and in-service related bonding quality reduction on the mode-I fracture toughness of composite bonded joints for aeronautical use. *Composites Part B: Engineering*, 45(1):556–564, 2013.
- [26] S Budhe, A Rodríguez-Bellido, J Renart, JA Mayugo, and J Costa. Influence of pre-bond moisture in the adherents on the fracture toughness of bonded joints for composite repairs. *International Journal of Adhesion and Adhesives*, 49:80–89, 2014.
- [27] BRK Blackman, BB Johnsen, AJ Kinloch, and WS Teo. The effects of pre-bond moisture on the fracture behaviour of adhesively-bonded composite joints. *The Journal of Adhesion*, 84(3):256–276, 2008.
- [28] E Moutsompegka, KI Tserpes, P Polydoropoulou, C Tornow, M Schlag, K Brune, B Mayer, and S Pantelakis. Experimental study of the effect of pre-bond contamination with de-icing fluid and ageing on the fracture toughness of composite bonded joints. *Fatigue & Fracture of Engineering Materials & Structures*, 40(10):1581–1591, 2017.
- [29] YC Lin, Xu Chen, HJ Zhang, and ZP Wang. Effects of hygrothermal aging on epoxy-based anisotropic conductive film. *Materials Letters*, 60(24):2958–2963, 2006.
- [30] A Cherdoud-Chihani, M Mouzali, and MJM Abadie. Study of crosslinking ams/dgeba system by ftir. *Journal of applied polymer science*, 69(6):1167–1178, 1998.
- [31] María González González, Juan Carlos Cabanelas, and Juan Baselga. Applications of FTIR on epoxy resins-identification, monitoring the curing process, phase separation and water uptake. In Theophile Theophanides, editor, *Infrared Spectroscopy-Materials Science, Engineering and Technology*.
- [32] Graham Beamson. High resolution XPS of organic polymers. *The Scienta ESCA 300 Database*, 1992.
- [33] D. Briggs and G. Beamson. High resolution XPS of organic polymers: The scienta esca300 database. *Journal of Chemical Education*, 70(A25), 1993.
- [34] E. Pretsch, P. Bühlmann, C. Affolter, E. Pretsch, P. Buhlmann, and C. Affolter. *Structure determination of organic*

- compounds*. Springer, 2000.
- [35] Andrey Krauklis and Andreas Echtermeyer. Mechanism of Yellowing: Carbonyl Formation during Hygrothermal Aging in a Common Amine Epoxy. *Polymers*, 10(1017):1–15, 2018.
- [36] Koji Nakanishi, Philippa H Solomon, et al. *Infrared absorption spectroscopy*. Holden-day, 1977.
- [37] A. S. Khan, H. Khalid, Z. Sarfraz, M. Khan, J. Iqbal, N. Muhammad, M.A. Fareed, and I.U. Rehman. Vibrational spectroscopy of selective dental restorative materials. *Applied Spectroscopy Reviews*, 52(6):507–540, 2017.
- [38] S. Musić, N. Filipović-Vinceković, and L. Sekovanić. Precipitation of amorphous SiO<sub>2</sub> particles and their properties. *Brazilian journal of chemical engineering*, 28(1):89–94, 2011.
- [39] S. Azarshin, J. Moghadasi, and Z. A Aboosadi. Surface functionalization of silica nanoparticles to improve the performance of water flooding in oil wet reservoirs. *Energy Exploration & Exploitation*, 35(6):685–697, 2017.
- [40] V. Baglio, A. Di Blasi, V. Antonucci, et al. FTIR spectroscopic investigation of inorganic fillers for composite dmfc membranes. *Electrochemistry communications*, 5(10):862–866, 2003.
- [41] Anderson J Bonon, Marcus Weck, Estevam A Bonfante, and Paulo G Coelho. Physicochemical characterization of three fiber-reinforced epoxide-based composites for dental applications. *Materials Science and Engineering: C*, 69:905–913, 2016.
- [42] Fredrick N Mutua, Peijie Lin, Jacob K Koech, and Yimin Wang. Surface modification of hollow glass microspheres. 2012.
- [43] GZ Xiao and MER Shanahan. Irreversible effects of hygrothermal aging on dgeba/dda epoxy resin. *Journal of Applied Polymer Science*, 69(2):363–369, 1998.
- [44] Cysne Barbosa, Ana Paula P. Fulco, Erick S.S. Guerra, Francisco K. Arakaki, Márcio Tosatto, Maria Carolina B. Costa, and José Daniel D. Melo. Accelerated aging effects on carbon fiber/epoxy composites. *Composites Part B: Engineering*, 110:298–306, 2017.
- [45] Aline Simar, Marco Gigliotti, Jean-Claude Grandidier, and Isabelle Ammar-Khodja. Decoupling of water and oxygen diffusion phenomena in order to prove the occurrence of thermo-oxidation during hygrothermal aging of thermosetting resins for RTM composite applications. *Journal of Materials Science*, 53(16):11855–11872, 2018.
- [46] A. Abdessalem, S. Tamboura, J. Fitoussi, H. Ben Daly, and A. Tcharkhtchi. Bi-phasic water diffusion in sheet molding compound composite. *Journal of Applied Polymer Science*, 137(7):1–12, 2020.
- [47] DM Choi, CK Park, K Cho, and CE Park. Adhesion improvement of epoxy resin/polyethylene joints by plasma treatment of polyethylene. *Polymer*, 38(25):6243–6249, 1997.
- [48] Rongzhi Li, Lin Ye, and Yiu-Wing Mai. Application of plasma technologies in fibre-reinforced polymer composites: a review of recent developments. *Composites Part A: Applied Science and Manufacturing*, 28(1):73–86, 1997.
- [49] David Gravis, Fabienne Poncin-Epaillard, and Jean-François Coulon. Correlation between the surface chemistry, the surface free energy and the adhesion of metallic coatings onto plasma-treated poly (ether ether ketone). *Applied Surface Science*, 501(144242), 2020.
- [50] Meng-Jiy Wang, You-Im Chang, and F Poncin-Epaillard. Acid and basic functionalities of nitrogen and carbon dioxide plasma-treated polystyrene. *Surface and Interface Analysis: An International Journal devoted to the development and application of techniques for the analysis of surfaces, interfaces and thin films*, 37(3):348–355, 2005.
- [51] GZ Xiao, M Delamar, and MER Shanahan. Irreversible interactions between water and DGEBA/DDA epoxy resin during hygrothermal aging. *Journal of applied polymer science*, 65(3):449–458, 1997.
- [52] Patrícia Alves, Susana Pinto, Hermínio C. de Sousa, and Maria Helena Gil. Surface modification of a thermoplastic polyurethane by low-pressure plasma treatment to improve hydrophilicity. *Journal of Applied Polymer Science*, 122(4):2302–2308, 2011.
- [53] M. Pizzorni, E. Lertora, C. Gambaro, C. Mandolino, M. Salerno, and M. Prato. Low-pressure plasma treatment of CFRP substrates for epoxy-adhesive bonding: an investigation of the effect of various process gases. *The International Journal*

- of *Advances Manufacturing Technology*, 102(9-12):3021–3035, 2019.
- [54] Yu Ren, Chunxia Wang, and Yiping Qiu. Influence of aramid fiber moisture regain during atmospheric plasma treatment on aging of treatment effects on surface wettability and bonding strength to epoxy. *Applied Surface Science*, 253(23):9283–9289, 2007.
- [55] G Borcia, N Dumitrascu, and G Popa. Influence of helium-dielectric barrier discharge treatments on the adhesion properties of polyamide-6 surfaces. *Surface and Coatings Technology*, 197(2-3):316–321, 2005.
- [56] Nicolas Vandencastele and François Reniers. Surface characterization of plasma-treated ptfе surfaces: an oes, xps and contact angle study. *Surface and Interface Analysis: An International Journal devoted to the development and application of techniques for the analysis of surfaces, interfaces and thin films*, 36(8):1027–1031, 2004.
- [57] Frédéric Piasecki. *Résines polyépoxydes nanostructurées aux propriétés d’adhésion et à la tenue au vieillissement améliorées*. PhD thesis, Université de Bordeaux-I, Laboratoire de Chimie des Polymères Organiques, Bordeaux, 2013.
- [58] M. Déroiné. *Étude du vieillissement de biopolymères en milieu marin*. Phd thesis, Université de Bretagne-Sud, Laboratoire d’ingénierie de matériaux de Bretagne, Lorient, France, 2014.
- [59] V. Berthé, L. Ferry, J.C. Bénézet, and A. Bergeret. Ageing of different biodegradable polyesters blends mechanical and hydrothermal behavior. *Polymer Degradation and Stability*, 95(3):262–269, 2010.
- [60] Jalal El Yagoubi, Gilles Lubineau, Frederic Roger, and Jacques Verdu. A fully coupled diffusion-reaction scheme for moisture sorption–desorption in an anhydride-cured epoxy resin. *Polymer*, 53(24):5582–5595, 2012.
- [61] L. Poussines. *Développement de nouveaux matériaux pour l’infusion de composites*. Phd thesis, Institut National Polytechnique de Toulouse, Laboratoire Génie de Production (INP-ENIT), Tarbes, France, 2012.